Thalamocortical NMDA conductances and intracortical inhibition can explain cortical temporal tuning

Anton E. Krukowski[1,2,6] and Kenneth D. Miller[2,3,4,5]

Biophysics Graduate Program[1], W. M. Keck Center for Integrative Neuroscience[2], Department of Physiology[3], Department of Otolaryngology[4] and Sloan-Swartz Center for Theoretical Neurobiology at UCSF[5], University of California, San Francisco, California 94143-0444, USA

[6] Present address: NASA Ames Research Center, Mail Stop 262-2, Moffett Field, California 94035-1000, USA

Correspondence should be addressed to K.D.M. and A.E.K. (ken@phy.ucsf.edu and akrukowski@mail.arc.nasa.gov)

Cells in cerebral cortex fail to respond to fast-moving stimuli that evoke strong responses in the thalamic nuclei innervating the cortex. The reason for this behavior has remained a mystery. We study an experimentally motivated model of the thalamic input-recipient layer of cat primary visual cortex that accounts for many aspects of cortical orientation tuning. In this circuit, inhibition dominates over excitation, but temporal modulations of excitation and inhibition occur out of phase with one another, allowing excitation to transiently drive cells. We show that this circuit provides a natural explanation of cortical low-pass temporal frequency tuning, provided *N*-methyl-D-aspartate (NMDA) receptors are present in thalamocortical synapses in proportions measured experimentally. This suggests a new and unanticipated role for NMDA conductances in shaping the temporal response properties of cortical cells, and suggests that common cortical circuit mechanisms underlie both spatial and temporal response tuning.

Cells in the primary visual cortex (V1) of cats[1–5] and monkeys[6,7] fail to respond to fast-moving stimuli that evoke strong responses in the lateral geniculate nucleus (LGN)[8–11], the source of visual inputs to V1. This is exemplified by the temporal frequency tuning of V1 neurons, determined by studying neuronal response to a drifting sinusoidal luminance grating of the neuron's preferred spatial frequency and orientation, as a function of the grating's temporal frequency. Cortical cells cease responding, with increasing temporal frequency at frequencies to which LGN cells respond vigorously. Similar temporally low-pass behavior is seen in other cortical areas such as the primary auditory[12] and somatosensory[13] cortices. The origin of this temporal behavior remains an outstanding puzzle for the understanding of cerebral cortical circuitry.

We previously introduced a circuit model of cat V1 layer 4, the input-recipient layer of the cortex. The structure of this model was determined by developmental learning rules and constraints from intracellular studies. We showed that this model could account for many attributes of the orientation tuning of cortical neurons, including the invariance of this tuning to changes in stimulus contrast[14]. Here we report that this same circuit model provides a natural and unexpected explanation for cortical temporal frequency tuning that also suggests a new role for NMDA receptors in determining cortical temporal response properties.

In the proposed circuit, the 'feedforward' inhibition (LGN-driven, but mediated by cortical interneurons) and feedforward excitation received by a cell are spatially opponent; that is, excitation and inhibition are driven by stimuli of opposite light/dark polarity at any given point in the visual field, as observed experimentally[15,16]. As a result, a drifting sinusoidal grating of the preferred orientation and spatial frequency alternately evokes excitation and inhibition, allowing the cell to respond periodically (for example, **Fig. 1b**, top). However, feedforward inhibition is stronger overall than feedforward excitation, so that simultaneous activation of all LGN inputs yields net inhibition (consistent with the massive inhibition observed experimentally in cortex in response to shocks to LGN[17]). Thus, cortical cells can only respond when a stimulus evokes sufficient temporal modulation of feedforward excitation and/or inhibition to avoid their simultaneous activation. Therefore, our modeling task is to determine, in terms of the biophysics of the cells and synapses, at what temporal frequency excitation and/or inhibition become effectively demodulated, and under what conditions this can account for the observed temporal frequency tuning of cortical cells.

Various biophysical mechanisms act on the feedforward inputs to a cortical cell to reduce their ability to follow fast modulations. One such mechanism is the cell's membrane time constant, which acts to low-pass filter the cellular voltage response. However, we will find, in agreement with others[18,19], that cortical membrane time constants (15–24 ms at rest[16]) are too short to account for cortical temporal frequency tuning. Another demodulating mechanism is the time course of synaptic conductances: each input spike to a cell is convolved with this time course to produce a synaptic current, and this convolution acts as a low-pass filter. Specifically, slow synaptic conductances, such as those mediated by NMDA receptors, will demodulate the input at relatively low frequencies.

We show that, if the thalamocortical synapses include the proportion of NMDA receptors observed in thalamocortical slices[20,21], our model circuit suffices to explain the low-pass temporal frequency tuning of visual cortex. However, there are conflicting data as to the strength of NMDA receptors in thalamocortical synapses[20–29] (see Discussion). Accordingly, we

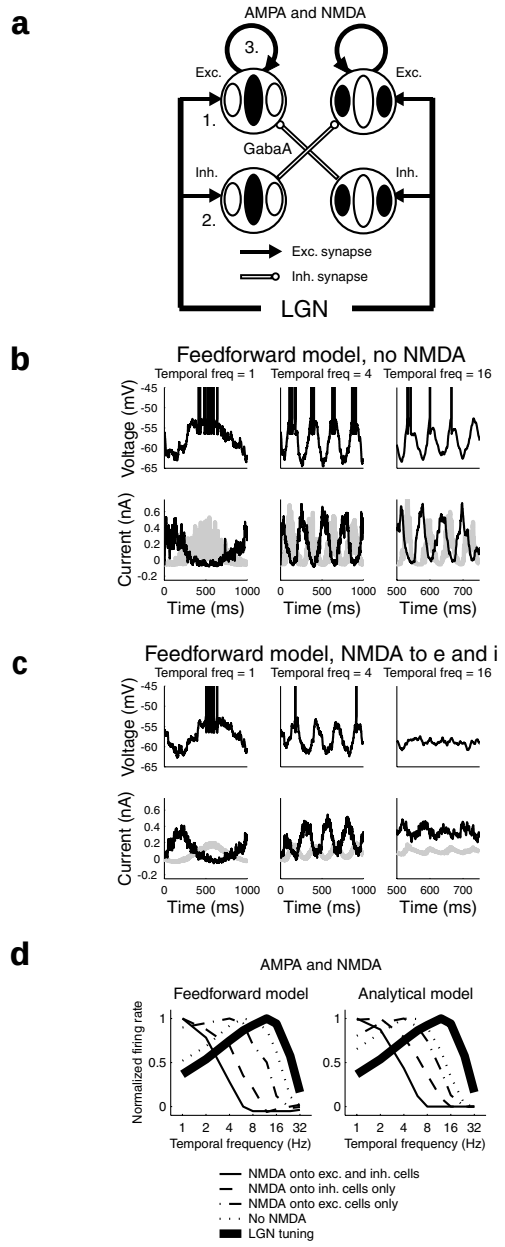

Fig. 1. Overview of the model and its behavior. (**a**) Model circuit. Top, two excitatory cells; bottom, two inhibitory cells. Receptive fields (RFs), white, ON subregions; dark, OFF subregions. All four illustrated RFs are meant to be centered on the same retinotopic position. In the actual model, cells of all preferred orientations and spatial phases and with multiple retinotopic positions exist, and connectivity is assigned probabilistically. The cartoon indicates the dominant or most probable connections in the model. Cells tend to receive input from ON-center LGN cells with centers overlying ON subregions, and from OFF-center cells overlying OFF subregions. Excitatory cells tend to connect to other cells of similar preferred orientation and similar absolute spatial phase (that is, ON subregions of the two cells tend to overlap in visual space, and similarly for OFF subregions). Inhibitory cells tend to connect to other cells of similar preferred orientation and opposite absolute spatial phase[15,16]. We examine the effect of NMDA receptors in three different sets of connections: the thalamocortical connections onto excitatory cortical cells (1), the thalamocortical connections onto inhibitory cortical cells (2), and the intracortical connections between excitatory cells (3). (**b–d**) Results in feedforward version of the model, meaning that there are no excitatory-to-excitatory connections (no connections of type 3, neither AMPA nor NMDA). (**b**, **c**) An example of excitatory and inhibitory input to a single cell at three different temporal frequencies. In both (**b**) and (**c**), voltage traces are on top, current traces are on bottom. Gray, excitatory current traces (AMPA plus NMDA); black, inhibitory current traces ($GABA_A$). (**b**) No NMDA. (**c**) With NMDA in thalamocortical synapses onto both excitatory and inhibitory cells; the percentage of NMDA is set so that the integrated excitatory current at spike-threshold voltage is 90% NMDA-mediated, which is slightly less than reported in thalamocortical synapses at the oldest ages studied[21] (see Methods). (**d**) Temporal frequency tuning in the feedforward model (left) and in a simple analytical model (right). Each figure compares the temporal frequency tuning of the mean firing rates of the LGN inputs in the model, taken from experimental measurements[11], to the tuning of the cortical cells under four conditions: no NMDA in any of the thalamocortical synapses, 90% NMDA in thalamocortical synapses onto excitatory cells only, 90% NMDA in thalamocortical synapses onto inhibitory cells only, and 90% NMDA onto both excitatory and inhibitory cells. Parameter sets with no synaptic depression and no feedback excitation are used in (**b–d**).

examine the dependence of the degree of low-pass shift on this strength. We also examine additional circuit mechanisms that can act on comparable time scales—feedback excitation[18,19] and synaptic depression[30]—and determine whether and how they might alter our results. Finally, we examine the effects on temporal tuning of developmental changes in the timing of NMDA conductances[21,31], changes that are strikingly correlated with developmental shifts in cortical temporal tuning[1,32].

Results

The model we study is identical to that of our previous study[14] except that NMDA conductances were not considered in that work. We model a network of conductance-based integrate-and-fire cells, representing a sheet of simple cells in layer 4 of cat V1. These cells are excited by light or by dark in alternating, oriented subregions of visual space, known as ON or OFF subregions, respectively (**Fig. 1a**). Both geniculocortical and intracortical excitation are driven by light in ON subregions or dark in OFF subregions. Inhibition, mediated by cortical inhibitory interneurons, is spatially opponent to or 'push-pull' with excitation, that is, it is driven by dark in a cell's ON subregion or light in a cell's OFF-subregion[15,16].

We first consider the effect of including NMDA in thalamocortical connections in a purely feedforward circuit model, that is, with the excitatory-to-excitatory connections (**Fig. 1a**) turned off. (For simplicity, we will use 'NMDA' in place of 'NMDA-receptor-mediated conductances' or 'NMDA-receptor-mediated.') We examine this simplified model first because it contains the main effect. We subsequently examine the involvement of several factors, including intracortical excitatory connections, that can modulate this effect. The percentage of NMDA in thalamocortical synapses is strongest in very young animals and decreases rapidly during development[21]. Because we are modeling temporal tuning in mature animals, we set this percentage to that measured in thalamocortical synapses *in vitro* at the oldest ages studied[21].

Traces from a single cell in the feedforward model show that without NMDA (**Fig. 1b**), the excitation and inhibition are well modulated, and the cell is therefore able to respond at high as well as low temporal frequencies. This means that cellular time constants cannot account for cortical low-pass behavior. (Without synaptic input, we use time constants of 20 ms for excitatory cells[16,33], and 11.9 ms for inhibitory cells[33].) In contrast, when NMDA is present in thalamocortical synapses to both excitatory and inhibitory cells (**Fig. 1c**), its long decay-time constant demodulates the input at higher temporal frequencies, and the domi-

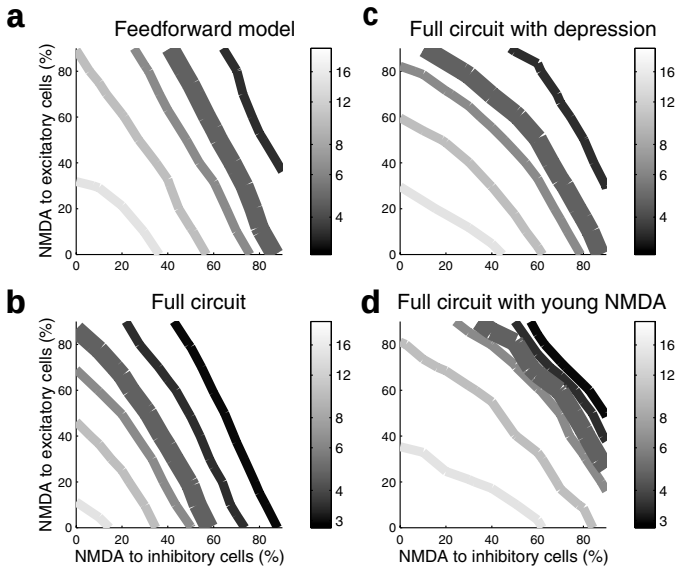

Fig. 2. Quantitation of model temporal tuning and main parameter dependence. Contour plot of temporal frequency cutoffs (frequencies at which response equals half the maximal response) shown as a function of percentage of total integrated current at spike-threshold voltage mediated by NMDA in thalamocortical synapses onto excitatory cells (vertical axes) and onto inhibitory cells (horizontal axes). The levels of gray of the contours represent the value of the temporal frequency cutoff, as shown in the grayscale bar; contours are shown for 3 (**b**, **d** only), 4, 6, 8, 12 and 16 Hz. The thicker line at 6 Hz represents a typical experimental value of temporal frequency cutoffs for cat simple cells[1–5]. (**a**) Parameter set with no synaptic depression with no feedback excitation. (**b**) Parameter set with no synaptic depression and with feedback excitation. (**c**) Parameter set with synaptic depression and feedback excitation. (**d**) Slow (young) NMDA with synaptic depression and feedback excitation.

nance of the mean inhibition over the mean excitation prevents the cell from firing.

Thus, NMDA-induced demodulation of the thalamocortical input induces low-pass shifts in cortical temporal frequency tuning relative to LGN tuning, whereas little or no shift occurs in the absence of NMDA (**Fig. 1d**). Although the strongest shifts are observed when NMDA is present in thalamocortical connections to both excitatory and inhibitory cells, significant shifts also occur if NMDA is present only in connections to excitatory or connections to inhibitory cells. The case of NMDA connections only to excitatory cells is of particular interest, because experimental evidence shows that inhibitory cortical cells receive less NMDA input than excitatory cells[28,29].

We tested the intuition that thalamocortical NMDA acts as a low-pass filter on the feedforward conductances, by comparing the results of the feedforward model to a simple analytical model. (Details are available on the *Nature Neuroscience* web site.) In the analytical model, we consider the responses of a single simple cell that receives direct excitatory input from the LGN and inhibitory input from a single simple cell that has an identical receptive field, but is of opposite spatial phase. Synaptic inputs are modeled as injected currents rather than as time-varying conductances, and spike rates are modeled as a linear function of the cell's membrane potential above a fixed threshold. Despite the simplicity of this model, the resultant temporal frequency tuning curves are remarkably similar to those of the feedforward model (**Fig. 1d**). This indicates that the essential reason for the cortical low-pass behavior in the feedforward model can indeed be understood as resulting from the low-pass filtering of the input by the time course of the NMDA conductances.

Having illustrated the basic mechanism, we quantitatively assay model results, which allows comparison with experimental results. To quantify the degree of shift in the temporal frequency tuning curves, we use a measure often used experimentally: the high-frequency cutoff, defined as the temporal frequency at which the mean spike-rate response is reduced to 50% of the peak. Because the actual percentages of NMDA conductances in geniculocortical synapses remains unclear, and because it is unlikely that many NMDA conductances exist in geniculocortical synapses onto inhibitory cells[28,29], we parametrically examine the dependence of model behavior on these percentages.

We first examine this dependence for the feedforward model (**Fig. 2a**). Each contour line represents a constant high-frequency cutoff. The thicker line represents a temporal frequency cutoff of 6 Hz, which is a representative experimental cutoff value for cortical cells[1–5]. In the feedforward model, this cutoff value cannot be achieved unless NMDA mediates roughly 50% or more of thalamocortical input to inhibitory cells.

We next examine the effect of including feedback excitation (the excitatory-to-excitatory connections in **Fig. 1a**), which amplifies responses to effective input. We assume that feedback synapses are predominantly mediated by NMDA, as suggested by previous studies[20,34]. Because of this dominance of NMDA, the feedback excitatory connections selectively amplify lower temporal frequencies, and do not significantly affect responses to higher frequencies. Given moderate to high levels of thalamocortical NMDA, this lowers the temporal frequency cutoff, and in particular, allows the 6-Hz cutoff to be achieved even if there is no NMDA in thalamocortical synapses onto inhibitory cells (**Fig. 2b**).

It has been suggested that feedback connections alone might yield shifts in cortical temporal tuning[18,19]. To test this, we examine the tuning using varying proportions of NMDA in the feedback connections, in the presence or absence of NMDA in the thalamocortical connections (**Fig. 3**). When NMDA is present in thalamocortical synapses onto excitatory cells, NMDA in feedback synapses shifts the cutoff frequency toward lower temporal frequencies (**Fig. 3a** and **c**), as we have just seen. However, in the absence of NMDA in thalamocortical synapses, NMDA in feedback synapses simply amplifies low-frequency responses, without altering temporal frequency cutoffs (**Fig. 3b** and **c**). Thus, NMDA in the feedback synapses can augment a low-pass shift induced by thalamocortical NMDA, but cannot induce such a shift by itself.

Short-term synaptic depression is another physiological property of cortical synapses that exists experimentally and that acts on appropriate time scales to potentially affect temporal frequency tuning[35,36]. We find that synaptic depression actually acts as a weak high-pass filter, moving the tuning slightly to higher frequencies, but the low-pass effect of NMDA still dominates (**Fig. 2c**, compare with **Fig. 2b**).

Finally, we examine the effects of the change observed developmentally in the decay time of NMDA conductances. Young animals show a markedly slower NMDA decay[31], and show lower temporal frequency cutoffs (for example, 4 Hz in 4-week-old cats in a study that found 7-Hz cutoffs in adult cats[1]). Furthermore, there are other strong developmental parallels

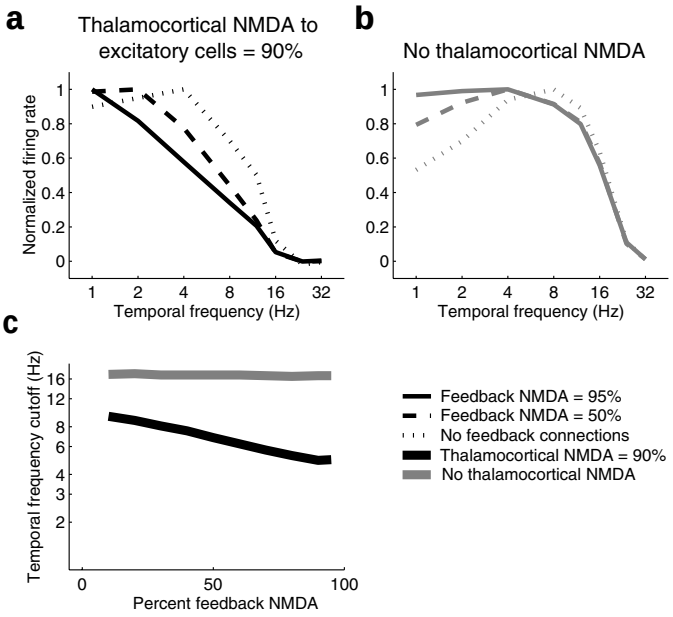

Fig. 3. Temporal frequency tuning of the model with different levels of NMDA in the feedback excitatory connections. (**a**, **b**) Temporal frequency tuning curves (normalized so that maximal response is 1) for two levels of feedback NMDA and for no feedback connections at all. (**a**) With 90% NMDA in the thalamocortical connections onto excitatory cells. (**b**) No NMDA in thalamocortical connections. (**c**) High-frequency cutoff versus percentage NMDA in feedback excitatory connections. Gray trace is with no thalamocortical NMDA (taken from **b**). Black trace is with 90% thalamocortical NMDA onto excitatory cells (taken from **a**). Parameter set with no synaptic depression and with feedback excitation.

between NMDA decay rates and temporal frequency cutoffs (see Discussion). We assume both feedback and thalamocortical NMDA are of the young form, and examine the resulting temporal frequency cutoffs (**Fig. 2d**). Two effects compete. The young NMDA causes demodulation at lower frequencies in thalamocortical synapses, lowering cutoff frequencies. However, it also reduces the effectiveness of feedback amplification at moderate frequencies, reducing peak responses and thereby raising the cutoff frequency. For lower levels of thalamocortical NMDA, the net effect is that temporal tuning curves are either unchanged or slightly shifted to higher cutoffs by young NMDA. However, if thalamocortical NMDA levels are high in connections to both inhibitory and excitatory neurons, the slower NMDA significantly reduces the temporal frequency cutoff (**Fig. 2d**; compare **Fig. 2c**). Because high levels of NMDA are found in young animals[21,22,37], this regime of high thalamocortical NMDA onto both excitatory and inhibitory neurons may be appropriate for young animals expressing slow NMDA receptors.

Discussion

We have demonstrated that a simple model of cortical circuitry that has previously accounted for the contrast invariance of orientation tuning of layer 4 simple cells[14] can robustly account for the low-pass shift in temporal frequency tuning from the LGN to the cortex, provided only that NMDA-mediated conductances are present in thalamocortical synapses in proportions measured experimentally[21]. Such a shift in temporal tuning seems to be a general trend in the difference between thalamic and cortical cells[12,13], which suggests that this may be a general role of NMDA in thalamocortical connections in various species and various cortical regions. Consistent with experimental evidence that inhibitory cortical cells receive less NMDA input than excitatory cells[28,29], we find that thalamocortical NMDA predominantly or solely onto excitatory cells is sufficient to account for the degree of low-pass shift observed in cat V1 cells. As we will discuss below, our results suggest a causal connection between two developmental changes—changes in the timing of NMDA conductances, and in cortical temporal tuning—that follow one another in a remarkably parallel fashion.

Strength of thalamocortical NMDA

It has been reported that NMDA makes little contribution to visual responses in layer 4 cells in mature cat V1 (ref. 22), suggesting there is little NMDA in mature thalamocortical synapses. (Similar results have also been seen in other cortical areas[23,24].) However, *in vitro* studies suggest that even though NMDA levels in thalamocortical synapses decrease with age, a significant NMDA component remains into maturity[20,21]. Furthermore, *in vivo* studies that used global blockade of NMDA[25,26] rather than local iontophoresis[22] found dramatic reductions in visual activation throughout visual cortex, and one study using iontophoresis found reductions in visual response in at least some layer 4 cells[27]. Although we do not know how to reconcile these conflicting reports, a key prediction of our model is that thalamocortical synapses onto excitatory cells in mature cat V1 should have levels of NMDA similar to that observed in rat somatosensory thalamocortical slices in the most mature animals studied[21].

However, there is an alternative possibility. If a significant fraction of inhibitory current is mediated by $GABA_B$ receptors, which cause a slow inhibitory conductance, feedforward inhibition would be demodulated and results would resemble those seen in the present model when only thalamocortical synapses onto inhibitory cells contain NMDA (**Fig. 2**). Because $GABA_B$-mediated currents are only rarely seen in *in vitro* studies of cortical inhibitory synapses[38], we have regarded this scenario as less likely than the NMDA scenario. However, there is evidence of $GABA_B$ receptor involvement in cat V1 responses[39,40].

Developmental implications

Experimental evidence shows a strong correlation between developmental changes in cortical temporal frequency tuning and developmental changes in the timing of the decay of NMDA conductances. Cortical cells in kittens are tuned to lower temporal frequencies than in adults cats[1]. (LGN cells also show a developmental shift in temporal tuning, but the LGN shift is not as strong as the cortical shift[41].) NMDA-mediated EPSPs have longer decay-time constants in slices from young animals than from mature animals[21,31]. Both these developmental shifts are delayed by rearing animals under dark conditions[31,32]. Furthermore, after dark rearing, both recover within hours of exposure to light. Six-week-old dark-reared kittens will suddenly shift their temporal tuning toward the tuning of normally raised 6-week-old kittens with 6 hours of exposure to light[32]. In addition, the shift toward normal levels of NR2A subunits, which underlies the shift to shorter NMDA decay-time constants, occurs in dark-reared rats after as little as two hours light exposure[42].

The model suggests that this striking correlation might be causal: the developmental shift to faster NMDA may at least par-

tially underlie the developmental shift to higher temporal frequencies. In the model, high NMDA onto both excitatory and inhibitory neurons was needed for the slower NMDA found in young animals to lower temporal frequency cutoffs. Thus, the model also suggests that developmental decreases in the proportion of NMDA, particularly in thalamocortical synapses onto inhibitory cells, may be important in the developmental shift in temporal frequency tuning. In normal development, the proportion of NMDA decreases in parallel with the shift in decay-time constant[21,22,31,37]. Dark rearing maintains the contribution of NMDA receptors to visual responses seen in young animals[43,44], and so this high-thalamocortical-NMDA regime may also apply to dark-reared animals. However, nothing is yet known specifically about the proportion of NMDA in thalamocortical synapses onto inhibitory neurons at any developmental time.

Other experimental predictions

The connection between NMDA receptor subtype and temporal frequency tuning could be tested by studying temporal tuning in mature mice that have been genetically engineered to overexpress the NR2B subunit of the NMDA receptor[45]. These animals, though mature, show the slow decay and large amplitude of NMDA of normal young animals. Our model suggests that these mature animals might also show the slow cortical temporal frequency tuning of normal younger animals.

A natural test of the model would seem to be to block NMDA receptors and examine the resulting change in temporal frequency tuning. Unfortunately, we have found that because such a block reduces excitatory input in response to any temporal frequency, NMDA blockade may either raise or lower temporal frequency cutoffs, depending on parameters. (Details are available on the *Nature Neuroscience* web site.) An ideal (but currently unfeasible) experiment would be to substitute AMPA for NMDA, thus reducing the demodulating effect of NMDA without reducing total excitation; this should raise temporal frequency cutoffs.

The model predicts that some cortical layer 4 inhibitory cells will be active in response to the highest temporal frequencies to which LGN cells respond well, because cortically induced inhibition prevents the remaining cortical cells from responding to this LGN drive. Consistent with this, in several areas of rabbit cortex, suspected interneurons follow much higher frequencies of peripheral stimulation than efferent (excitatory) neurons[46–48].

Both owl monkeys[7] and macaque monkeys[6] show a low-pass shift in temporal tuning between LGN and layer 4 of V1, and a further shift between layer 4 and subsequent cortical layers. If input demodulation also cuts off responses in layer 2/3, then a higher proportion of NMDA may exist in synapses from layer 4 to layers 2/3 than in thalamocortical synapses. The cutoffs reported in macaque[6] were very high: 41 Hz in LGN and 30 Hz in V1 layer 4. This V1 cutoff could be induced by cellular membrane time constants, and is much higher than would be expected from NMDA-induced demodulation. Thus, we would predict that macaque layer 4 cells either do not receive dominant opponent inhibition, so that demodulation does not cut off responses, or else have little NMDA in their thalamocortical synapses. However, it is also possible that these high cutoffs involve differences in anesthesia rather than species differences[6].

Alternative models

Two previous studies have proposed that feedback excitation could selectively amplify low-velocity responses, thus converting band-pass LGN tuning to low-pass cortical tuning[18,19]. One study[18] suggested this would arise through slow synaptic conductances in feedback synapses, and because strong feedback excitation would increase the effective time constant. The other study[19] proposed that spike-rate adaptation would make the feedback stronger for weaker inputs. We have found that selective low-frequency amplification indeed occurs in our model when feedback synapses include slow NMDA conductances, but that this cannot explain the lower high-frequency cutoff of cortical versus LGN temporal tuning. Instead, slow conductances in thalamocortical synapses, along with a push–pull circuit in which inhibition is dominant, are crucial.

An alternative explanation of low-pass behavior in some cortical systems might involve synaptic depression. For example, if synapses are depressed after each presynaptic spike for some period τ, then it might be possible to see a loss of responses to frequencies greater than $1/\tau$. However, this will be parameter dependent in a complicated way. We have found that synaptic depression with a τ of 99 ms actually shifts tuning to slightly higher frequencies. Another modeling study[30] found that depression with a τ of 300 ms induced a slight shift toward lower frequencies, but in that study, the temporal tuning was primarily due to a cellular time constant assumed to be 30 ms (larger than typically observed at rest in cortex[16]).

Implications for cortical processing

We have shown that the low-pass temporal behavior of cerebral cortex can be understood from the combination of two elements. First, the circuitry of layer 4 must be such that feedforward inhibition dominates feedforward excitation, and effective stimuli evoke excitation and inhibition that are separated in time. There is much evidence supporting this in layer 4 of both cat V1 (refs. 15–17) and rodent whisker barrel (somatosensory) cortex[49]. These circuit properties ensure that temporal demodulation of the input will prevent responses. Second, there must be significant slow synaptic conductances in feedforward excitatory inputs (NMDA mediated) and/or feedforward inhibitory inputs ($GABA_B$ receptor mediated) to cause the excitatory and/or inhibitory inputs to demodulate at higher temporal frequencies. If the proportion of NMDA-mediated conductances observed in thalamocortical slices from somatosensory cortex[21] is present in thalamocortical synapses onto excitatory cells, this is sufficient. However, given the conflicting evidence discussed above, it is this second point that is most in need of further experimental testing. Although we have studied the specific circuit proposed in our previous study[14], any circuit with these two properties should give similar results.

This work proposes a simple solution to the long-standing puzzle in cortical physiology of why cortical cells do not respond to fast stimuli that drive their inputs well. A related puzzle has concerned orientation tuning in V1: because LGN inputs are not orientation tuned, they are driven well by stimuli oriented orthogonal to a cortical cell's preferred orientation. Why doesn't the cortical cell respond to such stimuli? We are proposing that these two seemingly unrelated puzzles have the same solution. In our study of the application of the present model circuit to orientation tuning[14], we pointed out that drifting gratings of different orientations evoke the same mean LGN input to a cortical cell, and differ only in the degree of temporal modulation in that input. In response to a preferred-orientation stimulus, a cell's LGN inputs all modulate their firing rates in synchrony, so the total LGN input is strongly modulated. As the orientation is moved away from the preferred, a cell's LGN inputs become increasingly desynchronized in their firing rate modulations, and so the total LGN input becomes demodulated. We showed that, given a circuit with dominant, spatially opponent inhibition, the orientation tuning cut off at an orienta-

tion for which the input was sufficiently demodulated. This orientation was roughly the same at any contrast, thus explaining the contrast-invariance of orientation tuning. Thus, we are proposing that orientation cutoffs and temporal frequency cutoffs have a common origin in more general principles of cortical layer 4: the circuit is dominated by inhibition, so that only out-of-phase temporal modulations of excitation and inhibition can drive cortical cells; therefore, stimuli become ineffective when they fail to evoke sufficient temporal modulation of the input.

Methods

The model used in this study is in almost all essential details identical to the 'computational' model described previously[14], except that NMDA receptors and synaptic depression were not considered in that study. We review here the basic elements of our model; full details of differences from our previous study[14] are available on the *Nature Neuroscience* web site.

Model architecture. The model consists of a grid of 40×40 excitatory and 20×20 inhibitory cortical simple cells, representing a 2/3 mm $\times$ 2/3 mm patch of cortex and $0.75° \times 0.75°$ in visual angle. The receptive field (RF) of each cell was determined by a Gabor function, with retinotopic center progressing linearly across the grid (with each inhibitory RF center aligned with every other excitatory cell), preferred orientation assigned according to an optically measured cortical map from cat V1, and spatial phase assigned randomly to each cell. The Gabor functions used the 'broadly tuned' receptive field parameters of our previous study[14], which were chosen to make intracellular voltage modulations match the measured orientation tuning width of the voltage modulations of cortical simple cells.

Input to the model cells came from a set of 30×30 grids of LGN X-cells, four superposed grids of ON-center and four superposed grids of OFF-center cells, with ON and OFF lattices offset by 1/2 lattice spacing. The grids covered $6.8° \times 6.8°$ of the visual field. Thalamocortical connections to each cortical cell were determined by probabilistic sampling from the cell's Gabor function, with positive (negative) regions converted to a probability of connection from an ON- (OFF-) center cell with corresponding RF center.

Intracortical connections were also determined probabilistically, with the probability of connection of any two cortical cells depending on the correlation between their sets of thalamocortical inputs. The probability of an excitatory connection was a monotonically increasing function of this correlation, whereas the probability of an inhibitory connection was a monotonically increasing function of the negative of this correlation. Thus, excitatory cells tended to project to cells with which they were most correlated, whereas inhibitory cells tended to project to cells with which they were most anticorrelated.

Determining cell activities. An LGN cell's firing rate was determined as the sum of a sinusoidal modulation at the same temporal frequency as the stimulus and with phase determined by the cell's RF center position, and a background firing rate (10 Hz for ON cells, 15 Hz for OFF cells), followed by setting negative rates to zero (rectification). The size of the sinusoidal modulation for a given grating was chosen so that after rectification, the first harmonic (F1) of the LGN responses matched the data of an experimental study[11] for X-cell response to the given contrast and temporal frequency. Times of LGN action potentials were then determined by generation of Poisson processes from the time-dependent firing rates.

Cortical cells were modeled as single-compartment, conductance-based integrate-and-fire neurons with biophysical parameters for excitatory and inhibitory neurons matched to experimental data[33] for regular-spiking and fast-spiking neurons, respectively.

Conductance models. Time course of AMPA, $GABA_A$ and adaptation conductances were each modeled as a difference of single exponentials, as described previously[14]. The decay of the NMDA conductance was described by a double exponential with a fast (63-ms) and a slow (200-ms) time constant, with amplitudes A_f and A_s respectively; the ratio A_f:A_s was 0.88:0.12 in adults, and 0.1:0.9 in young animals[31]. The voltage dependence of the NMDA conductance was taken from a published model[50]. The voltage used for this dependence was the voltage the cell would have if it did not spike, which we call V_{shadow}; this was done to avoid discontinuities in conductance at spikes as well as to take account of the location of NMDA conductances in dendrites. With this model of voltage dependence, the NMDA channels were 35.5% open at the model spike threshold voltage, –52.5 mV. In response to a high-contrast optimal grating, V_{shadow} reached a peak of approximately –46 mV, where the NMDA channels were 43.8% open.

The relative strength of NMDA and AMPA conductances in excitatory synapses can be described in one of two ways. The NMDA/AMPA amplitude ratio, as reported by an experimental study[21], is the ratio of the amplitude of NMDA EPSCs with the cell held at +40 mV to the amplitude of AMPA EPSCs with the cell held at –90 mV. Alternatively, one can specify the %NMDA integrated current, which is the percent of the temporally integrated current (that is, of the total charge transfer) through excitatory conductances that is mediated by NMDA conductances, when the postsynaptic cell is clamped at the spike-threshold voltage of –52.5 mV. Even for relatively modest NMDA/AMPA amplitude ratios, the integrated current is dominated by NMDA, due to the long NMDA decay-time constants (see *Nature Neuroscience* web site). An experimental study[21] reports an NMDA/AMPA amplitude of 0.30 for the oldest thalamocortical slices studied (8 to 14 postnatal days) which corresponds to 91.2% of the integrated current mediated by NMDA. We have accordingly used 90% NMDA as our default for full strength of NMDA in thalamocortical synapses.

The strengths of the synaptic and adaptation conductances were set as in our previous study[14], but some changes were needed to compensate for the effects of NMDA conductances and synaptic depression. (Full details, including our definitions of parameter sets, are available on the *Nature Neuroscience* web site.) Changes in the proportion of NMDA were implemented so that the total synaptic strength (total integrated current at threshold voltage) remained constant; only the percentage of this total integrated threshold current that is mediated by NMDA versus AMPA was altered.

We modeled synaptic depression using a model with two parameters[35]: f ($0 \le f \le 1$), the factor by which the efficacy of a synapse is scaled immediately after a spike, and τ, the time constant of an exponential decay back to maximum efficacy. We used the following parameters. For thalamocortical synapses, τ = 99 ms and f = 0.563; for intracortical excitatory synapses, τ = 57 ms and f = 0.875. (Experimental sources for these choices are discussed on the *Nature Neuroscience* web site.) Synaptic depression was not included in the inhibitory synapses.

Simulations. A 'blank screen' was run for one second preceding each stimulus presentation to equilibrate the network. Stimulus presentations were for one second. Stimulus-driven or background responses were determined from the second half-second of the stimulus or background, respectively. This allowed the network to first achieve steady state, which, when including NMDA, took on the order of a few hundred milliseconds. Responses were measured as stimulus minus background response. Tuning curves show the mean response over the pool of excitatory cells with preferred orientation ± 2.5° about the stimulus orientation. (This bin included 35 excitatory cells and 10 inhibitory cells.) The cutoff temporal frequency was determined by taking the mean response for these excitatory cells at a series of temporal frequencies (1, 2, 4, 6, 8, 12, 16, 24 and 32 Hz) and then using cubic spline interpolation to find the lowest frequency above the preferred frequency at which the response was half maximal.

Acknowledgements

We thank T. Troyer for discussions and L. Stone for comments on the manuscript. Supported by a Howard Hughes Medical Institute predoctoral fellowship (A.E.K.) and by RO1EY001 from the National Eye Institute (K.D.M.).

Note: Supplementary information is available on the Nature Neuroscience web site (http://neurosci.nature.com/web_specials).

Received 31 October 2000; Accepted 5 February 2001

1. DeAngelis, G. C., Ohzawa, I. & Freeman, R. D. Spatiotemporal organization of simple-cell receptive fields in the cat's striate cortex. I. General characteristics

and postnatal development. *J. Neurophysiol.* **69**, 1091–1117 (1993).
2. Holub, R. A. & Morton-Gibson, M. Response of visual cortical neurons of the cat to moving sinusoidal gratings: response-contrast functions and spatiotemporal interactions. *J. Neurophysiol.* **46**, 1244–1259 (1981).
3. Movshon, J. A., Thompson, I. D. & Tolhurst, D. J. Spatial and temporal contrast sensitivity of neurones in areas 17 and 18 of the cat's visual cortex. *J. Physiol. (Lond.)* **283**, 101–120 (1978).
4. Saul, A. B. & Humphrey, A. L. Temporal-frequency tuning of direction selectivity in cat visual cortex. *Vis. Neurosci.* **8**, 365–372 (1992).
5. Ikeda, H. & Wright, M. J. Spatial and temporal properties of sustained and transient neurones in area 17 of the cat's visual cortex. *Exp. Brain Res.* **22**, 363–383 (1975).
6. Hawken, M. J., Shapley, R. M. & Grosof, D. H. Temporal-frequency selectivity in monkey visual cortex. *Vis. Neurosci.* **13**, 477–492 (1996).
7. O'Keefe, L. P., Levitt, J. B., Kiper, D. C., Shapley, R. M. & Movshon, J. A. Functional organization of owl monkey lateral geniculate nucleus and visual cortex. *J. Neurophysiol.* **80**, 594–609 (1998).
8. Derrington, A. M. & Fuchs, A. F. Spatial and temporal properties of X and Y cells in the cat lateral geniculate nucleus. *J. Physiol. (Lond.)* **293**, 347–364 (1979).
9. Hamamoto, J., Cheng, H., Yoshida, K., Smith, E. L. & Chino, Y. M. Transfer characteristics of lateral geniculate nucleus X-neurons in the cat: effects of temporal frequency. *Exp. Brain Res.* **98**, 191–199 (1994).
10. Saul, A. B. & Humphrey, A. L. Spatial and temporal response properties of lagged and nonlagged cells in cat lateral geniculate nucleus. *J. Neurophysiol.* **64**, 206–224 (1990).
11. Sclar, G. Expression of "retinal" contrast gain control by neurons of the cat's lateral geniculate nucleus. *Exp. Brain Res.* **66**, 589–596 (1987).
12. Creutzfeldt, O., Hellweg, F. C. & Schreiner, C. Thalamocortical transformation of responses to complex auditory stimuli. *Exp. Brain Res.* **39**, 87–104 (1980).
13. Simons, D. J. Temporal and spatial integration in the rat SI vibrissa cortex. *J. Neurophysiol.* **54**, 615–635 (1985).
14. Troyer, T. W., Krukowski, A. E., Priebe, N. J. & Miller, K. D. Contrast-invariant orientation tuning in cat visual cortex: thalamocortical input tuning and correlation-based intracortical connectivity. *J. Neurosci.* **18**, 5908–5927 (1998).
15. Ferster, D. Spatially opponent excitation and inhibition in simple cells of the cat visual cortex. *J. Neurosci.* **8**, 1172–1180 (1988).
16. Hirsch, J. A., Alonso, J. M., Reid, R. C. & Martinez, L. M. Synaptic integration in striate cortical simple cells. *J. Neurosci.* **18**, 9517–9528 (1998).
17. Ferster, D. & Jagadeesh, B. EPSP–IPSP interactions in cat visual cortex studied with in vivo whole-cell patch recording. *J. Neurosci.* **12**, 1262–1274 (1992).
18. Maex, R. & Orban, G. A. A model circuit for cortical temporal low-pass filtering. *Neural Comput.* **4**, 932–945 (1992).
19. Suarez, H., Koch, C. & Douglas, R. Modeling direction selectivity of simple cells in striate visual cortex within the framework of the canonical microcircuit. *J. Neurosci.* **15**, 6700–6719 (1995).
20. Gil, Z. & Amitai, Y. Adult thalamocortical transmission involves both NMDA and non-NMDA receptors. *J. Neurophysiol.* **76**, 2547–2554 (1996).
21. Crair, M. C. & Malenka, R. C. A critical period for long-term potentiation at thalamocortical synapses. *Nature* **375**, 325–328 (1995).
22. Fox, K., Sato, H. & Daw, N. The location and function of NMDA receptors in cat and kitten visual cortex. *J. Neurosci.* **9**, 2443–2454 (1989).
23. Armstrong-James, M., Welker, E. & Callahan, C. A. The contribution of NMDA and non-NMDA receptors to fast and slow transmission of sensory information in the rat SI barrel cortex. *J. Neurosci.* **13**, 2149–2160 (1993).
24. Salt, T. E., Meier, C. L., Seno, N., Krucker, T. & Herrling, P. L. Thalamocortical and corticocortical excitatory postsynaptic potentials mediated by excitatory amino acid receptors in the cat motor cortex in vivo. *Neuroscience* **64**, 433–442 (1995).
25. Kasamatsu, T. *et al.* Roles of N-methyl-D-aspartate receptors in ocular dominance plasticity in developing visual cortex: re-evaluation. *Neuroscience* **82**, 687–700 (1998).
26. Miller, K. D., Chapman, B. & Stryker, M. P. Visual responses in adult cat visual cortex depend on N-methyl-D-aspartate receptors. *Proc. Natl. Acad. Sci. USA* **86**, 5183–5187 (1989).
27. Hagihara, K., Tsumoto, T., Sato, H. & Hata, Y. Actions of excitatory amino acid antagonists on geniculo-cortical transmission in the cat's visual cortex. *Exp. Brain Res.* **69**, 407–416 (1988).
28. Ling, D. S. & Benardo, L. S. Recruitment of $GABA_A$ inhibition in rat neocortex is limited and not NMDA dependent. *J. Neurophysiol.* **74**, 2329–2335 (1995).
29. Angulo, M. C., Rossier, J. & Audinat, E. Postsynaptic glutamate receptors and integrative properties of fast-spiking interneurons in the rat neocortex. *J. Neurophysiol.* **82**, 1295–1302 (1999).
30. Chance, F. S., Nelson, S. B. & Abbott, L. F. Synaptic depression and the temporal response characteristics of V1 cells. *J. Neurosci.* **18**, 4785–4799 (1998).
31. Carmignoto, G. & Vicini, S. Activity-dependent decrease in NMDA receptor responses during development of the visual cortex. *Science* **258**, 1007–1011 (1992).
32. Gary-Bobo, E., Przybyslawski, J. & Saillour, P. Experience-dependent maturation of the spatial and temporal characteristics of the cell receptive fields in the kitten visual cortex. *Neurosci. Lett.* **189**, 147–150 (1995).
33. McCormick, D. A., Connors, B. W., Lighthall, J. W. & Prince, D. A. Comparative electrophysiology of pyramidal and sparsely spiny stellate neurons of the neocortex. *J. Neurophysiol.* **54**, 782–806 (1985).
34. Feldmeyer, D., Egger, V., Lubke, J. & Sakmann, B. Reliable synaptic connections between pairs of excitatory layer 4 neurones within a single 'barrel' of developing rat somatosensory cortex. *J. Physiol. (Lond.)* **521**, 169–190 (1999).
35. Abbott, L. F., Varela, J. A., Sen, K. & Nelson, S. B. Synaptic depression and cortical gain control. *Science* **275**, 220–224 (1997).
36. Tsodyks, M. V. & Markram, H. The neural code between neocortical pyramidal neurons depends on neurotransmitter release probability. *Proc. Natl. Acad. Sci. USA* **94**, 719–723 (1997).
37. Catalano, S. M., Chang, C. K. & Shatz, C. J. Activity-dependent regulation of NMDAR1 immunoreactivity in the developing visual cortex. *J. Neurosci.* **17**, 8376–8390 (1997).
38. Thomson, A. M. & Destexhe, A. Dual intracellular recordings and computational models of slow inhibitory postsynaptic potentials in rat neocortical and hippocampal slices. *Neuroscience* **92**, 1193–1215 (1999).
39. Douglas, R. J. & Martin, K. A. A functional microcircuit for cat visual cortex. *J. Physiol. (Lond.)* **440**, 735–769 (1991).
40. Allison, J. D., Kabara, J. F., Snider, R. K., Casagrande, V. A. & Bonds, A. B. $GABA_B$-receptor-mediated inhibition reduces the orientation selectivity of the sustained response of striate cortical neurons in cats. *Vis. Neurosci.* **13**, 559–566 (1996).
41. Cai, D., DeAngelis, G. C. & Freeman, R. D. Spatiotemporal receptive field organization in the lateral geniculate nucleus of cats and kittens. *J. Neurophysiol.* **78**, 1045–1061 (1997).
42. Quinlan, E. M., Olstein, D. H. & Bear, M. F. Bidirectional, experience-dependent regulation of N-methyl-D-aspartate receptor subunit composition in the rat visual cortex during postnatal development. *Proc. Natl. Acad. Sci. USA* **96**, 12876–12880 (1999).
43. Fox, K., Daw, N., Sato, H. & Czepita, D. The effect of visual experience on development of NMDA receptor synaptic transmission in kitten visual cortex. *J. Neurosci.* **12**, 2672–2684 (1992).
44. Czepita, D., Reid, S. N. & Daw, N. W. Effect of longer periods of dark rearing on NMDA receptors in cat visual cortex. *J. Neurophysiol.* **72**, 1220–1226 (1994).
45. Tang, Y. P. *et al.* Genetic enhancement of learning and memory in mice. *Nature* **401**, 63–69 (1999).
46. Swadlow, H. A. Efferent neurons and suspected interneurons in S-1 vibrissa cortex of the awake rabbit: receptive fields and axonal properties. *J. Neurophysiol.* **62**, 288–308 (1989).
47. Swadlow, H. A. Efferent neurons and suspected interneurons in second somatosensory cortex of the awake rabbit: receptive fields and axonal properties. *J. Neurophysiol.* **66**, 1392–1409 (1991).
48. Swadlow, H. A. Efferent neurons and suspected interneurons in motor cortex of the awake rabbit: axonal properties, sensory receptive fields, and subthreshold synaptic inputs. *J. Neurophysiol.* **71**, 437–453 (1994).
49. Pinto, D. J., Brumberg, J. C. & Simons, D. J. Circuit dynamics and coding strategies in rodent somatosensory cortex. *J. Neurophysiol.* **83**, 1158–1166 (2000).
50. Jahr, C. E. & Stevens, C. F. Voltage dependence of NMDA-activated macroscopic conductances predicted by single-channel kinetics. *J. Neurosci.* **10**, 3178–3182 (1990).